Eur. Phys. J. B **16**, 593–600 (2000)

THE EUROPEAN PHYSICAL JOURNAL B

EDP Sciences

Electronic instabilities in the quasi-two-dimensional conducting monophosphate tungsten bronzes $K_xP_4W_8O_{32}$ ($0.75 < x < 2$)

S. Drouard[1], D. Groult[2], J. Dumas[1,a], R. Buder[1], and C. Schlenker[1]

[1] Laboratoire d'Études des Propriétés Électroniques des Solides, CNRS, BP 166, 38042 Grenoble Cedex 9, France
[2] Laboratoire CRISMAT[b], ISMRA-Université de Caen, 14050 Caen Cedex, France

Received 25 February 2000

Abstract. The monophosphate tungsten bronzes $K_xP_4W_8O_{32}$ are quasi-two-dimensional conductors. The parent compound $P_4W_8O_{32}$ shows two charge density wave instabilities (CDW). The layered structure of the doped compounds contains pseudo hexagonal tunnels stabilised by the insertion of potassium for $0.75 < x < 2$. In order to study the role of the band filling in the CDW instabilities, we have performed resistivity, magnetoresistance, Hall effect, thermopower and specific heat measurements on the doped compounds with $0.8 < x < 1.94$. Anomalies at a temperature T_c depending on x appear on all the transport properties. From transport data, we have obtained a phase diagram $T_c(x)$ which shows surprisingly a maximum at 170 K for $x = 1.3$. In the whole range of temperature studied (4.2 K–300 K), the transport properties of $K_xP_4W_8O_{32}$ show a change for $x \approx 1.3$. The diagram $T_c(x)$ is discussed in term of non-monotonous behaviour for the density of states *versus* the energy and in relation to previous X-ray studies. The transitions in $K_xP_4W_8O_{32}$ do not seem to be conventional Peierls instabilities in contrast with those observed in pure $P_4W_8O_{32}$.

PACS. 71.45.Lr Charge-density-wave systems – 72.15.Gd Galvanomagnetic and other magnetotransport effects

1 Introduction

Low-dimensional metallic oxides have been the subject of extensive studies for several decades in relation with their particular transport properties associated with two types of electronic instabilities: either a Peierls type transition toward a charge density wave (CDW) state [1–3] or a superconducting instability. Their history goes back to approximately 30 years ago, when the transition-metal-layered dichalcogenides were studied, mostly in relation to their strongly anisotropic anomalous conducting properties [4]. The mechanism of the Peierls instability in the quasi-two-dimensional (2D) conductors is related to the so-called nesting properties of the Fermi Surface (FS) [2, 3]. In an ideal 1D metal, the FS, being composed of two parallel planes separated by a vector $2k_F$, is totally destroyed by the Peierls transition (k_F is the Fermi wave vector). This so-called perfect nesting induces a metal-insulator transition. For the quasi-2D conductors, the FS is more complex and only a part of the FS is nested. This incomplete nesting gives rise to partial gap openings on the Fermi surface. In this case electron or hole pockets are left on the FS by the Peierls transition and a metal-metal transition is observed.

In this context, among the large family of metallic quasi-two-dimensional inorganic conductors, the monophosphate tungsten bronzes $(PO_2)_4(WO_3)_{2m}$ (MPTB), with values of m ranging from 4 to 14, have now been extensively studied [2,5,6,9]. The crystal structure of these series of compounds [7,8] is built with perovskite ReO_3-type infinite layers of WO_6 octahedra. The layers are connected together *via* PO_4 tetrahedra creating pentagonal tunnels (MPTBp). Two successive slabs are related by a 2_1-fold axis. Since the $5d$ conduction electrons are located in the WO_6 layers, the electronic properties are quasi-2D. The lattice is orthorhombic: the c parameter increases with m while a and b are only weakly dependent on it. The parameter m is thus related to the thickness of the $[WO_3]$-types slabs and also to the average number of conduction electrons per W: $2/m$. The number of conduction electrons per primitive cell is always four, independent on m. However the low-dimensional character is expected to change with the thickness of the WO_6 slabs. These compounds are therefore of interest since by changing m, the low-dimensional character can be modified without changing the conduction band filling. The monophosphate tungsten bronzes $(PO_2)_4(WO_3)_{2m}$ show CDW instabilities at critical temperature depending on m. Recent studies show that the critical temperature increases with m [9]. Let us note that the compound

[a] e-mail: dumas@lepes.polycnrs-gre.fr
[b] CNRS UMR 6508

$m = 7$ is the only member which shows a superconducting transition below 0.3 K in the CDW state [10].

Band structure calculations have been performed on $(PO_2)_4(WO_3)_{2m}$ ($m = 4, 6$) by Canadell and Wangbo using a tight binding extended Hückel method in a 2D approximation. In these approximations, three bands are found crossing the Fermi level [11]. Nesting properties appear on the resulting FS obtained from the superposition of these three sheets. These properties have been related to the so-called hidden nesting [12] due to the presence of infinite chains of WO_6 octahedra along the **a** and $(\mathbf{a} \pm \mathbf{b})$ axis. Therefore the FS can be described as the superposition of three quasi-1D FS's. Transport measurements performed on $P_4W_8O_{32}$ show two CDW instabilities characterised by a metal-metal transition at $T_{p1} = 80$ K and $T_{p2} = 52$ K [13]. X-ray diffuse scattering studies, showing satellite peaks which appear at T_{p1} and T_{p2}, allow the determination of the two incommensurate CDW wave vectors: ($q_1 = (0.33, 0.295, ?)$ and $q_2 = (0.34, 0, ?)$) [14]. Respectively these experimental values are very roughly consistent with two of the nesting vectors of the calculated Fermi surface.

As noticed above, in the series $(PO_2)_4(WO_3)_{2m}$, the number of conduction electron per unit cell, therefore the band filling, is invariant with m. Until now, only the influence of the low dimensional character, which increases with m, has been studied. However by inserting alkaline elements in a monophosphate tungsten bronze for a fixed value of m, one can change the band filling without changing the dimensionality of the compound. For the $K_x(PO_2)_4(WO_3)_{2m}$ family, the average conduction electron density is expected to be $(4 + x)/2m$ since the outer electron of the potassium should be transferred to the conduction band. The carrier density can be then modified without changing strongly the crystal structure.

This article reports studies performed on the $m = 4$ member. Structural data obtained on the compounds $K_xNa_yP_4W_8O_{32}$ lead to the determination of a phase diagram [15]. The phase diagram shows a great sensitivity of each phase to alkaline metal concentration. Four domains have been obtained. For very low values of this concentration, the MPTBp structure is stable. The largest domain corresponding to a single stable phase is found when the cation concentration is between 0.75 and 2. This phase is called MPTBh (h = hexagonal tunnels). The crystal structure of the MPTBh $K_xP_4W_8O_{32}$ single crystals, shown in Figure 1, is similar to that of $P_4W_8O_{32}$ [16]. However, in the K^+ doped compounds, the WO_6 strings in successive slabs are parallel. Due to this arrangement the structure is monoclinic and shows pseudo hexagonal tunnels (MPTBh) where the cations K^+ are located.

X-ray diffuse scattering experiments on $K_xP_4W_8O_{32}$ [17] show that there is no long-range order of potassium in the pseudo hexagonal tunnels and no correlation between neighbouring tunnels. The order of the K^+ ions increases with the increasing concentration. The potassium content $x = 2$ correspond to half of the sites occupied and to an order of the K^+ ions along the pseudo hexagonal tunnels. Band structure calculations have also been performed in this case using the refine structure of $K_{0.8}P_4W_8O_{32}$ [18]. They show Fermi surface nesting properties similar to those of $P_4W_8O_{32}$. Minor changes are predicted as x is varied if the crystal structure did not depend on x. Therefore these results predict a weak change of the nesting properties as a function of the potassium content.

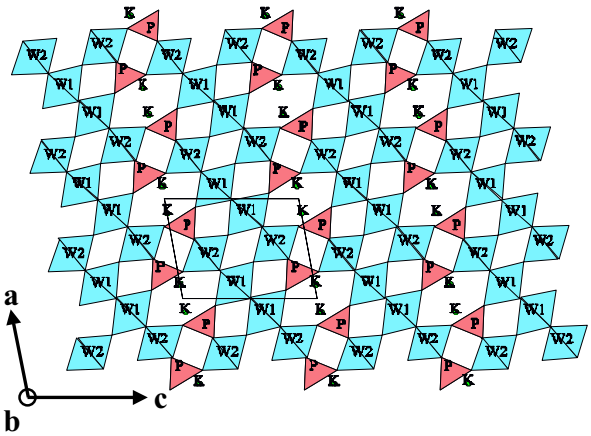

Fig. 1. Crystal structure of $K_xP_4W_8O_{32}$ in the *ac* plane (from Ref. [16]). The structure shows hexagonal tunnels where the K^+ ions are located.

We report in this article resistivity, magnetoresistivity, Hall effect and thermopower (TEP) measurements performed on $K_xP_4W_8O_{32}$ single crystals with hexagonal tunnels, with x varying from 0.8 to 1.94. Preliminary results have been published in reference [19] for three alkaline concentrations. We discuss the results in relation with band structure calculations and X-ray diffuse scattering data. In Section 2, the experimental techniques are described. Transport measurements results are reported in Section 3. Section 4 is devoted to the discussion of the normal state, the metal-metal transition and the low temperature state.

2 Experimental techniques

Powder samples of $K_x(PO_2)_4(WO_3)_{2m}$ are prepared. Mixture of $(NH_4)_2HPO_4$, WO_3 and K_2CO_3 in appropriate ratios were first heated in air at 600 °C for 12 h in order to decompose the phosphate and the carbonate. An adequate amount of metallic tungsten powder used as a reducing agent is then added to the decomposed initial mixture before grinding. The powder was then heated in an evacuated silica ampoule at 950 °C for 48 h and slowly cooled down to 25 °C. Single crystals are finally grown by the chemical transport technique. An amount of about 2 g of $K_xP_4W_8O_{32}$ polycrystalline sample is inserted in a quartz tube (20 cm long and 1.8 cm internal diameter), sealed under vacuum. After putting the tube in a horizontal furnace, a temperature gradient of about 10 °C/cm is applied along its length with the hot zone at 1200 °C and the cold zone at 1000 °C. The powder is held under these conditions for one week in order to grow single crystals at the cold zone. The tube is progressively cooled down

to 25 °C by successive steps at 1000 °C, 800 °C, 600 °C, 400 °C and 200 °C. Purple coloured crystals grow in the central part of the tube as plate-like needles and bars with largest sizes of $6 \times 3 \times 1$ mm^3. Details on crystal preparation are given in reference [8].

The K^+ concentration is obtained by energy dispersive X-ray spectrometry (EDS). The homogeneity is checked by measuring the EDS signal on three selected places of the crystal surface. The cell parameters of the single crystals were measured by X-ray powder diffraction patterns and the crystal quality checked by Weissenberg photographs. Films obtained with a Weissenberg camera show well-defined sharp spots, no apparent diffusion and no presence of twinning, which is rather rare for samples of this family. The observed monoclinic symmetry with b as the unique axis ($b = 5.3$ Å) and a β angle near 92.6° was confirmed later by diffractometric techniques [15]. The crystal are platelets parallel to the ab plane and perpendicular to the c^* axis.

For transport measurements, the contacts are made by thermal evaporation of silver on a surface cleaned in ammonia for about two hours. Gold wires ($\varnothing = 25$ μm) are attached on the evaporated areas by silver paste. The current is injected along the ab plane.

Resistivity and thermopower experiments have been performed in a He^4 cryostat over temperatures from 4.2 K to 300 K. The resistivity and the magnetoresistivity are measured by the four-probe technique. Thermopower data were obtained by an ac relaxation method: the ends of the crystal are fixed by two gold foils and glued with silver paste to the heating blocks, assuring a good thermal contact. An alternating thermal gradient is applied across the sample (max ± 1 K). The experiment is entirely computer controlled.

Magnetoresistance and Hall effect have been measured in a He^4 cryostat equipped with a superconducting coil providing magnetic fields up to 7.5 T. The magnetic field was perpendicular to the ab plane. The Hall voltage was obtained from the difference of the transverse voltage in a magnetic field of 6 T for the two field orientations.

Specific heat has been measured on the largest single crystals (> 5 mg), between 4.2 K and 30 K, with a home built microcalorimeter, using a relaxation technique.

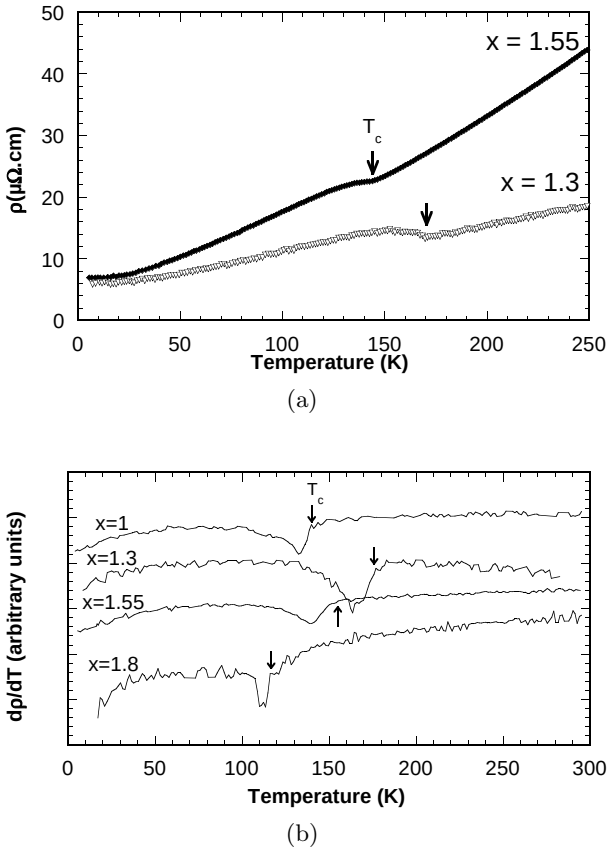

Fig. 2. (a) Resistivity curves $\rho(T)$ of $K_xP_4W_8O_{32}$ for $x = 1.3$ and 1.55. (b) Derivative $d\rho/dT$ *vs.* temperature for $K_xP_4W_8O_{32}$ for different values of x.

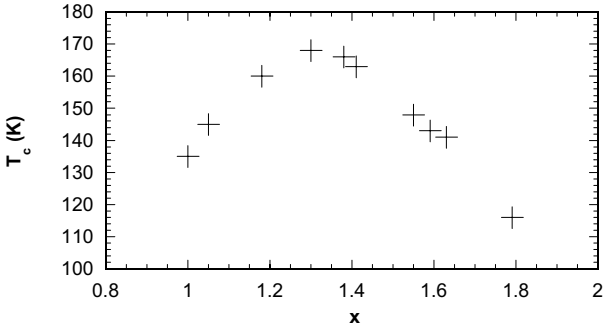

Fig. 3. Transition temperature *vs.* x for $K_xP_4W_8O_{32}$.

3 Experimental results

3.1 Resistivity vs. temperature and magnetoresistance

The in-plane resistivity ρ has been measured as a function of the temperature for several compositions ($0.86 \leq x \leq 1.94$) between 4.2 K and 300 K has been measured. $\rho(T)$ increases with temperature and is characteristic of a metal behaviour. However, for $1 \leq x \leq 1.8$, the curves $\rho(T)$ show an anomaly at a temperature T_c marked by a minimum followed by a bump and a decrease at lower temperature. The amplitude of this bump decreases as x increases. Typical $\rho(T)$ curves are given in Figure 2a. A more accurate determination of T_c is obtained by plotting the derivative $d\rho/dT$ *vs.* T as shown in Figure 2b. The $\rho(T)$ curves are similar to those observed for the low m compounds of the family $(PO_2)_4(WO_3)_{2m}$ showing metal-metal transitions due to Peierls transitions. In the doped compounds the temperatures $T_c(x)$ are found to be between 110 K and 170 K and therefore higher than the transition temperatures observed on $P_4W_8O_{32}$. With increasing x, the resistivity anomalies become weaker: for $x = 1.94$ no anomaly has been observed. The curve of T_c as a function of the potassium content x is shown in Figure 3. One notes that $T_c(x)$ increases from $T_c = 135$ K

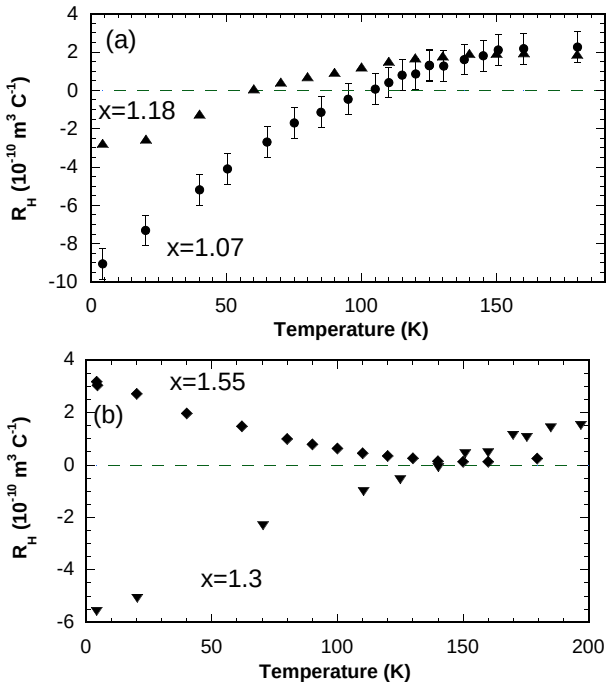

Fig. 4. Hall effect *vs.* temperature of $K_xP_4W_8O_{32}$: (a) x = 1.07 and 1.18; (b) $x = 1.3$ and 1.55.

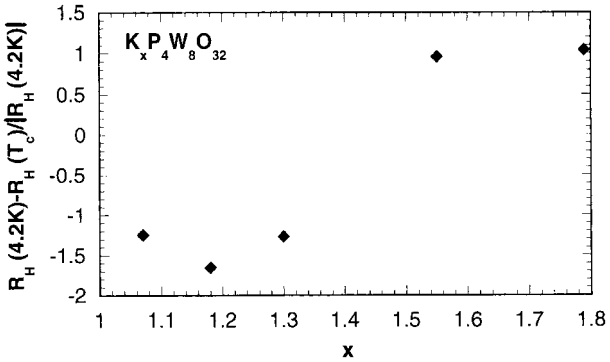

Fig. 5. $(R_H(4.2\text{ K})\text{-}R_H(T_c))/|R_H(4.2\text{ K})|$ *vs.* x for $K_xP_4W_8O_{32}$.

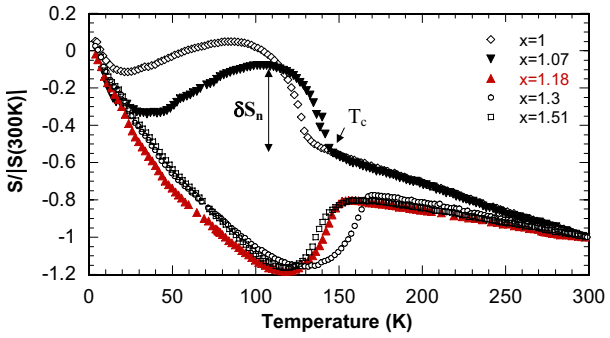

Fig. 6. Thermopower normalised to the absolute value at 300 K, $S/|S(300\text{ K})|$, *vs.* temperature of $K_xP_4W_8O_{32}$. $\delta S_n = \delta S/|S(300\text{ K})|$ (see text).

($x = 1$) to a maximum value of 170 K for $x = 1.3$, then decreases, reaching 110 K for $x = 1.8$.

We have previously reported resistivity measurements as a function of the magnetic field B, up to 7.5 T, at 4.2 K for different concentrations of K^+. A positive transverse magnetoresistance $\Delta R/R$ is observed in all cases. It increases quadratically with the magnetic field. For all values of x the magnetoresistance is of the order of 20% at 7.5 T [17]. The angular dependence of the magnetoresistance measured for $B = 7.5$ T at 4.2 K shows a cos θ law as expected for a quasi-2D compound.

3.2 Hall effect

Hall voltage has been measured between 4.2 K and 200 K for six values of x ($1 \leq x \leq 1.79$). Figure 4 shows the Hall coefficient R_H as a function of temperature for $x = 1.07$ and 1.18, and for $x = 1.3$ and 1.55 respectively. R_H is found to be approximately ten times smaller than in the case of $P_4W_8O_{32}$. In the high temperature state, $|R_H|$ is in the range of 10^{-10} m^3/C, which is close to the limit of sensitivity of the equipment. However R_H seems to be positive for $x \leq 1.3$. A change of slope is observed at the temperature T_c determined from resistivity measurements. Up to $x = 1.3$, R_H is negative at 4.2 K while for $x = 1.55$ and 1.79, R_H is positive at low temperatures. We have plotted the ratio $(R_H(4.2\text{ K})-R_H(T_c))/|R_H(4.2\text{ K})|$ *vs.* x in Figure 5. This ratio does not depend on possible errors on the sample thickness values. It has the same sign as that of the Hall coefficient at low temperature. One notes a change of behaviour for x between 1.3 and 1.5.

3.3 Thermopower

The curves of the thermopower normalised to the absolute value obtained at room temperature are shown in Figure 6 as a function of the temperature for different values of x. At high temperature, the Seebeck coefficient S is negative for all x and varies linearly with the temperature. Upon cooling, a strong change of slope is observed. Below the transition at T_c the curves show a bump. This change takes place at the same temperature as the onset of the anomaly on the resistivity curves. Below T_c, two kinds of behaviour are found as a function of the potassium concentration x: for $x < 1.15$, S increases with decreasing temperature while for $x > 1.15$, S become more negative. Figure 7 shows the slope $\Delta S/\Delta T$ of S *vs.* T in the normal state *versus* x and the difference δS between the minimum or maximum value of the TEP below T_c and S at T_c *vs.* x. One notes that the slope $\Delta S/\Delta T$ is strongly dependent on x for $x < 1.2$ and weakly above. A change of behaviour is also found below T_c: δS is positive for $x \leq 1.15$ and becomes negative for $x > 1.15$.

3.4 Specific heat

The specific heat C_p has been measured *vs.* temperature between 4.2 K and 25 K for three compounds $K_xP_4W_8O_{32}$ with $x = 1.07$, 1.25 and 1.6. The curves C_p/T *vs.* T^2

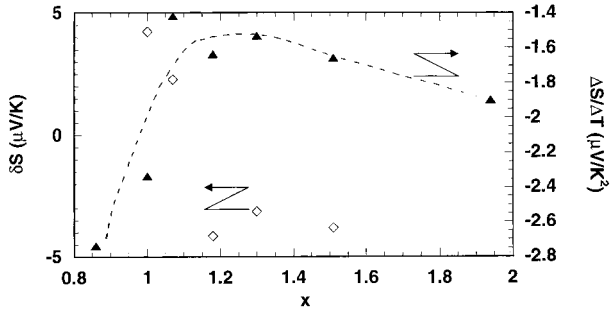

Fig. 7. Left scale (◊): difference between the thermopower at T_c and the extremum below T_c δS *vs.* x. Right scale (▲): slope of the thermopower, $\Delta S/T$, in the normal state *vs.* x.

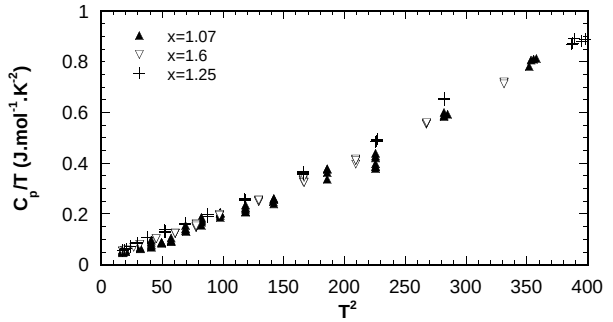

Fig. 8. Specific heat plotted as C_p/T *vs.* T^2 for $K_xP_4W_8O_{32}$ ($x = 1.07$; 1.25 and 1.6).

($T \leq 15$ K) are given in Figure 8. The results do not seem to depend significantly on the potassium concentration. A good fit according to the formula $C_p = \gamma T + \beta T^3$ is obtained for $T \leq 15$ K. From the value of β in equation (1):

$$\beta = \frac{12\pi^4 n_a k_B}{5\theta_D^3} \quad (1)$$

where n_a is the number of atoms per formula unit, one obtains a Debye temperature of the order of 350 ± 10 K for the three investigated compounds.

The specific heat of a sodium doped compound, $Na_1P_4W_8O_{32}$ has also been measured. This compound shows also a structure with hexagonal tunnels. Within the error bar, the curve C_p/T *vs.* T^2 is the same as for the $K_xP_4W_8O_{32}$ samples. These results suggest that the low temperature specific heat and therefore the Debye temperature do not depend on the filling of the hexagonal tunnels by the alkaline ions but only on the host structure.

4 Discussion

We will first discuss the properties of the normal metallic state, then the metal-metal transition, and finally the low temperature state.

4.1 Normal state

At high temperature, the compounds $K_xP_4W_8O_{32}$ ($0.8 < x < 1.94$) show a conventional metallic behaviour. From

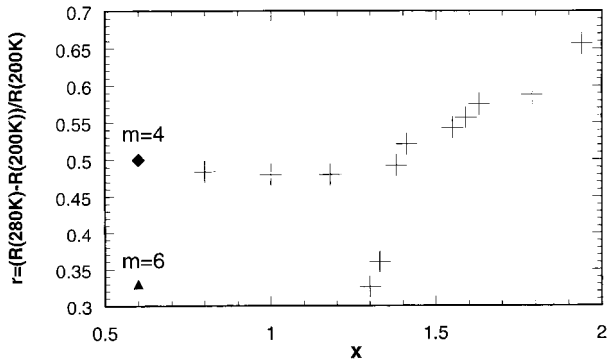

Fig. 9. Slope r of the resistivity in the normal state $[R(280\text{ K}) - R(200\text{ K})]/R(200\text{ K})$ for the pure $m = 4$ and $m = 6$ compounds and for $K_xP_4W_8O_{32}$ *vs.* x.

the resistivity data, one obtains the ratio $r = [R(280\text{ K}) - R(200\text{ K})]/R(200\text{ K})$ for various concentrations. This ratio is plotted for the pure compounds $m = 4$ and $m = 6$ and for the doped compounds in Figure 9. The curve $r(x)$ shows a minimum for $x = 1.3$. These results can be discussed in the framework of the Bloch-Gruneisen model [20] for the collisions of carriers with phonons. In this model, the resistivity is expected to be related to the Debye temperature θ_D as $\rho \propto T/\theta_D^2$. The Debye temperature have been found to be 276 K for the $m = 4$ compound and 237 K for the $m = 6$ one [21]. One notes that the ratio r is found to be 0.51 and 0.33 for the two compounds. These results cannot clearly be accounted for by the Bloch-Gruneisen model. Moreover, the Debye temperature θ_D does not depend sensitively on x for the doped compounds: $\theta_D \approx 350$ K, while r is changing with x. Again, this is inconsistent with the Bloch-Gruneisen result. Other mechanisms must therefore be responsible for the variation of r with x. They may involve a non-monotonous band filling [17].

Considering now the Hall effect data, one notes that in the normal state, the Hall coefficient is weaker than in the pure $m = 4$ parent compound. This may indicate that the doped compounds are more compensated metals [22] than the pure one. This compensation is due to comparable contributions of electron and hole type Fermi surface sheets. For values of $x \leq 1.3$, R_H is positive which indicates that hole pockets are dominant. For other values of x, $|R_H|$ is of the order of the experimental uncertainty and its sign cannot be determined unambiguously.

On the other hand the TEP values are negative at high temperature. The difference in sign of the dominant carriers, as obtained from Hall effect and TEP data, confirms that the $K_xP_4W_8O_{32}$ compounds are nearly compensated metal. This difference is not surprising and is found in other nearly compensated metals. In a crude two bands approach, the TEP is given by the relation:

$$S = \frac{\sigma_1 S_1 + \sigma_2 S_2}{\sigma_1 + \sigma_2} \quad (2)$$

where S_i is the contribution of the i-band and σ_i the corresponding conductivity ($\sigma_i = n_i e \mu_i$ where μ_i is

the mobility), while:

$$R_{\mathrm{H}} = \frac{R_{\mathrm{H}}\sigma_1^2 + R_{\mathrm{H}}\sigma_2^2}{(\sigma_1 + \sigma_2)^2} \tag{3}$$

where $R_{\mathrm{H}i}$ is the Hall coefficient of the i-band. In fact, the sign of the Hall coefficient is dominated mainly by the cyclotron properties and by electron trajectories along the section of the FS perpendicular to the magnetic field. On the other hand, the slope of the curve of the thermopower *vs.* temperature is related to the Fermi energy, or to the density of states at the Fermi level. Figure 7 shows that, in the normal state, this slope is dependent on x, with a change of behaviour for $x \approx 1.3$. For $x > 1.3$, it is nearly independent on x while for the smaller values of x, it increases with x. This suggests a change of the band filling mechanism above $x = 1.3$, which is not inconsistent with the Hall effect data in the normal state.

4.2 Metal-metal transition

The anomalies in the electrical resistivity, thermopower and Hall effect at a temperature T_{c} depending on x, establish that changes of the electronic properties occur at T_{c} and that a new metallic state is induced below T_{c}. The resistivity shows a metallic behaviour in both states. This indicates that there is only a partial nesting of the FS in the normal state and therefore that partial openings of gaps take place at the transition. The values of T_{c} found for $K_xP_4W_8O_{32}$, between 110 K and 170 K, are larger than the Peierls transition temperature of the pure $m = 4$ compound. The phase diagram $T_{\mathrm{c}}(x)$ showing a maximum of T_{c} for $x = 1.3$, is unexpected since in a simple system, one would expect a monotonous variation of the conduction band filling when x is increased. The observed behaviour is reminiscent of that found in high-T_{c} superconductors upon doping, where the superconducting transition temperature shows a maximum for a given value of the oxygen stoichiometry [23].

In order to discuss the phase diagram of $K_xP_4W_8O_{32}$, one has to take into account changes in the density of states at the Fermi energy and possibly changes in the electron-phonon interactions. Since the monophosphate tungsten bronzes exhibit hidden one-dimensionality, one may use, in an attempt to explain the results, the following mean field expression for the critical temperature valid in the 1D case:

$$k_{\mathrm{B}}T_{\mathrm{c}} = 2.28\varepsilon_{\mathrm{F}} \exp\left[\frac{-\hbar\omega_0(2k_{\mathrm{F}})}{\lambda^2 g(\varepsilon_{\mathrm{F}})}\right] \tag{4}$$

where $g(\varepsilon_{\mathrm{F}})$ is the density of states at the Fermi level. From this formula, T_{c} should increase when $g(\varepsilon_{\mathrm{F}})$ increases. For $x < 1.3$, $T_{\mathrm{c}}(x)$ would result from an increase of $g(\varepsilon_{\mathrm{F}})$ with x, as a consequence of band filling. This is consistent with a decrease of ρ with x at room temperature. For $x > 1.3$, the decrease of $T_{\mathrm{c}}(x)$ would be due to a decrease of $g(\varepsilon_{\mathrm{F}})$. This is again consistent with the observed increase of ρ *vs.* x at room temperature.

In this simple description, the curve $T_{\mathrm{c}}(x)$ could correspond to the existence of a maximum in the electronic density of states $g(\varepsilon)$ *vs.* ε, the Fermi level crossing the maximum when x is changed. This scenario is reminiscent of that invoked in the description of the dependence of the superconducting transition temperature upon doping [23] and based on a Van Hove singularity [24]. In our case, the maximum in the curve $g(\varepsilon)$ could be a consequence of the crossing of the Fermi level by several bands. In this model, the characteristic value $x = 1.3$ would correspond to the Fermi level located at the maximum of $g(\varepsilon)$. One should note that $x = 1.3$ corresponds roughly to 2/3 electron per W atom. However, the complicated band structure with three bands crossing the Fermi level make a more detailed interpretation difficult. Furthermore, the dependence of the electron-phonon coupling constant on x is unknown.

The TEP data at the transition corroborate a change of behaviour *vs.* x: for the low concentration of K^+ the Seebeck coefficient S shows a positive bump below T_{c} whereas a negative one is observed for $x > 1.15$. This indicates that for these concentrations of potassium, hole pockets on the FS are induced by the transition. These results showing a change in the band properties around $x \approx 1.3$ are not contradictory with the previous analysis. This phenomenon is reminiscent of the TEP data found for the quasi-two-dimensional purple bronzes AMo_6O_{17} as a function of the nature of the alkaline metal A (A = Na, K and Tl) [25]. In this case the electronic structure and also the nesting properties depend on nature of the alkaline ion.

From the structural point of view, X-ray studies show that satellites peaks appearing at the temperature T_{c} occur at the same commensurate value $\mathbf{q} = 0.5\mathbf{a}^*$ whatever x [17]. This is surprising since the modulation vector is expected to change with the FS and to be correlated to the band filling. This behaviour indicates that a lock-in by the lattice occurs at the transition whatever the value of x is.

4.3 Low temperature state

At low temperature, the resistivity is metallic-type and saturates below ≈ 15 K. This saturation value corresponds to the residual resistivity due to structural defects and impurities in the crystals. This residual resistivity does not seem to depend strongly on the K^+ concentration.

At low temperature, the sign of the Hall coefficient R_{H} depends on the K^+ concentration. Figure 5 shows that R_{H} is negative for $x \leq 1.3$ and changes sign for $1.3 < x < 1.55$. These results show that the sign of the dominant carriers left on FS by the transition, changes for $x \approx 1.3$.

A change of sign of the carriers *vs.* x below T_{c} is also found in the TEP data. For $x < 1.2$, the Seebeck coefficient S is close to zero and a weak negative bump is observed around 20 K. This weak value of S indicates a comparable contribution of the holes and of the electrons. The low temperature bump is probably due to phonon drag effects [26]. For $x \geq 1.2$, S is clearly negative, which

Table 1. Carriers concentrations at low temperature and mobilities extrapolated to 0 K for different K^+ concentrations.

x	1.18	1.3	1.55
$n = p$ (10^{20} cm^{-3})	4.9	9.8	10.2
μ (0 K) (cm^2 V^{-1} s^{-1})	654	702	607
ν (0 K) (cm^2 V^{-1} s^{-1})	623	586	674

indicates that electrons are dominant carriers at low temperatures. The effect of the phonon drag is not observed for $x \geq 1.2$ probably because it is hidden by the steep variation of the thermopower.

For a given value of x, the sign of the carriers as obtained by TEP and Hall effect are not in agreement. This confirms that the $K_xP_4W_8O_{32}$ compounds are nearly compensated metals. At low temperature, one may try to obtain some information on the FS and on the carrier concentration using combinated magnetoresistance *vs.* temperature and Hall effect data. One can analyse these data using the so-called two-band model. The usual approximations are valid if the magnetoresistivity $\Delta\rho/\rho$ follows a quadratic field dependence in low field. It should saturate at higher fields, except if the metal is fully compensated. R_H should be field independent in the limit of low fields. In the case of nearly full compensation, one may take the electron concentration n to be equal to the hole concentration p. In a rough approximation of only two bands and using the measured values of the conductivity, of R_H and of $\Delta\rho/\rho$, one may evaluate the carrier concentration and the mobilities of the electrons μ and of the holes ν using the formula given in reference [27]. For $n = p$ the formula for the resistivity, the magnetoresistance and the Hall effect are respectively:

$$\rho = \frac{1}{ne(\mu + \nu)} \tag{5}$$

$$\frac{\Delta\rho}{\rho} = \mu\nu B^2 \tag{6}$$

$$R_H = \frac{1}{ne}\frac{\nu - \mu}{\nu + \mu}\,. \tag{7}$$

The magnetoresistance decreases with increasing temperature and can be measured only up to 100 K. In this range of temperature ($T < T_c$), the partial gaps are already opened and the carriers concentrations n and p should not depend on the temperature. The results are shown in Figures 10a, b for the mobilities of $K_xP_4W_8O_{32}$ for the concentrations $x = 1.3$ and 1.55 respectively. The carriers concentrations are found to be approximately temperature independent. Their value as well as those of the mobilities extrapolated to 0 K are reported in Table 1. One may note that the values of n and p in the low temperature state of $K_xP_4W_8O_{32}$ are one order of magnitude larger than the $m = 4$ compound ($n \approx 4 \times 10^{19}$ cm^{-3}) [12]. This is consistent with the fact that the $m = 4$ compounds shows two successive Peierls transitions and that the loss of carriers is more important than in the doped compounds.

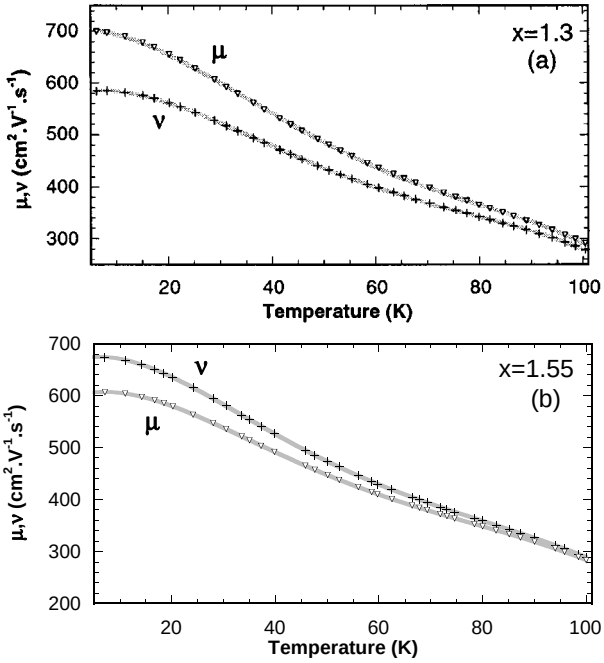

Fig. 10. Mobilities μ of electrons and ν of holes *vs.* temperature evaluated with a tow-bands model for $K_xP_4W_8O_{32}$: (a) $x = 1.3$; (b) $x = 1.55$.

The carrier mobilities decrease with increasing temperature. The mobilities of the electrons are larger than that of the holes for $x = 1.18$ and 1.3 and lower for $x = 1.55$. As expected, this model reflects a change of the electronic behaviour at $x \approx 1.3$. If we compare the values extrapolated to 0 K of the carriers mobilities of $K_xP_4W_8O_{32}$ and $P_4W_8O_{32}$, we find that they are one order of magnitude smaller in the doped compounds than in the $m = 4$ compound. This difference could be due to disorder of K^+ in the pseudo-hexagonal tunnels of $K_xP_4W_8O_{32}$ which might lower the mobilities of the carriers.

All the transport data obtained on $K_xP_4W_8O_{32}$ show that a change in the low temperature state occurs around $x = 1.3$. This is probably due to a change of the electronic structure *vs.* x. The low temperature state is similar to that observed for the $m = 4$ and $m = 6$ compounds. However this is not a conventional charge density wave instability since the modulation wave vector is commensurate and independent on x. We suggest that the corresponding wave vector is associated to a given band.

5 Conclusion

We have investigated by transport measurements the effect of the band filling on the electronic instabilities of the monophosphate tungsten bronzes $K_xP_4W_8O_{32}$. A new phase diagram $T_c(x)$ has been obtained. $T_c(x)$ is a non-monotonous function of the alkali metal concentration x, a maximum being observed for $x = 1.3$. The results have been discussed in terms of changes in the electronic density of states. For the low values of x ($x < 1.3$), an increase

with x of the density of states at the Fermi level $g(\varepsilon_F)$ induces an increase of T_c, while for $x > 1.3$ a decrease of $g(\varepsilon_F)$ may be responsible for the decrease of T_c with increasing x.

In the context of a Peierls-type transition, we assume that the density of states $g(\varepsilon)$ *vs.* ε shows a maximum. This would induce a maximum of the density of states at the Fermi level occurring at $x = 1.3$. Moreover, this complex mechanism appears to be associated to a lock-in by the lattice to a commensurate state.

Contrarily to the case of $P_4W_8O_{32}$, even though we observed similar behaviours in $K_xP_4W_8O_{32}$, the instabilities in the doped compounds do not seem to be conventional Peierls transitions since the modulation wave vector $2k_F$ is commensurate and does not depend on x. Hall effect and TEP measurements indicate that the bronzes $K_xP_4W_8O_{32}$ are nearly compensated metals and the opposite signs for the Hall coefficient R_H and the Seebeck coefficient S have to be related to the complex topology of the Fermi surface.

For a better understanding of the band filling mechanism, more accurate band calculations would be required. It would also be interesting to study other members of the family $A_x(PO_2)_4(WO_3)_{2m}$.

The authors would like to thank P. Foury, P. Labbé, J. Marcus, P. Roussel and E. Canadell for helpful discussions and for characterisation facilities provided by the CRISMAT laboratory.

References

1. R. Peierls, *Quantum Theory of Solids* (Oxford University Press, Oxford, 1955), p. 108.
2. *Physics and Chemistry of Low Dimensional Inorganic Conductors*, Vol. 354 of NATO-ASI, Series B: Physics, edited by C. Schlenker, J. Dumas, M. Greenblatt, S. Van Smalen (Plenum, New York, 1996).
3. *Density Waves in Solids*, edited by G. Gruner (Addison-Wesley, Reading, MA, 1994).
4. J.A Wilson, A.D. Yoffe, Adv. Phys. **18**, 193 (1969).
5. *Oxides Bronzes*, edited by M. Greenblatt, Int. J. Mod. Phys. B **7**, 4045 (1993).
6. C. Schlenker, C. Le Touze, C. Hess, A. Rötger, J. Dumas, J. Marcus, M. Greenblatt, Z.S. Teweldemedhin, A. Ottolenghi. P. Foury, J.P. Pouget, Synth. Met. **70**, 1263 (1995).
7. B. Domengès, F. Studer, B. Raveau, Mater. Res. Bull. **18**, 669 (1983).
8. Ph. Labbé, M. Goreaud, B. Raveau, J. Solid State Chem. **61**, 234 (1986).
9. C. Schlenker, C. Hess, C. Le Touze, J. Dumas, J. Phys. I France **6**, 2061 (1996); J. Dumas, U. Beierlein, S. Drouard, C. Hess, D. Groult, Ph. Labbé, P. Roussel, G. Bonfait, E. Gomez Marin, C. Schlenker, J. Solid State Chem. **147**, 320 (1999).
10. C. Hess, C. Schlenker, G. Bonfait, T. Ohm, C. Paulsen, J. Dumas, Z. Teweldemedhin, M. Greenblatt, J. Marcus, M. Almeida, Solid State Commun. **104**, 663 (1997).
11. E. Canadell, M. Whangbo, Phys. Rev. B **43**, 1894 (1990); Chem. Rev. **91**, 965 (1991); and in reference [5], p. 4005.
12. M.H. Whangbo, E. Canadell, P. Foury, J.P. Pouget, Science **252**, 96 (1991).
13. C. Hess, C. Schlenker, J. Dumas, M. Greenblatt, Z.S. Teweldemedhin, Phys. Rev. B **54**, 4581 (1996).
14. P. Foury, J.P. Pouget, Z.S. Teweldemedhin, E. Wang, M. Greenblatt, D. Groult, J. Phys. IV France **3**, C2-133 (1993) and in reference [5], p. 3973.
15. J.P. Giroult, M. Goreaud, Ph. Labbé, B. Raveau, J. Solid State Chem. **81**, 173 (1989).
16. P. Roussel, D. Groult, A. Maignan, Ph. Labbé, Chem. Mat. (to be published).
17. S. Drouard, P. Foury, P. Roussel, D. Groult, J. Dumas, J.P. Pouget, C. Schlenker, Synth. Met. **103**, 2636 (1999).
18. E. Canadell (private communication).
19. P. Roussel, D. Groult, C. Hess, Ph. Labbé, C. Schlenker, J. Phys. Cond. Mat. **9**, 7081 (1997).
20. J.M. Ziman, *Electrons and Phonons* (Oxford University Press, 1960), p. 364.
21. J. Lehmann, C. Schlenker, C. Le Touze, A. Rötger, J. Dumas, J. Marcus, Z.S. Teweldemedhin, M. Greenblatt, J. Phys. IV France **3**, C2-243 (1993).
22. A.B. Pippard, *Magnetoresistance in Metals* (Cambridge University Press, 1989).
23. C.N.R Rao, A.K. Ganguli, Physics C **9**, 235 (1994).
24. J. Labbé, Phys. Scri. T **29**, 82 (1989).
25. M. Tian, L. Chen, H. Sekine, J. Shi, R. Wang, Z. Mao, Y. Zhang, Phys. Let. A **234**, 477 (1997).
26. R.D. Barnard, *Thermoelectricity in Metals and Alloys* (Taylor & Francis, London, 1972).
27. W. Mercouroff, *La Surface de Fermi des métaux* (Masson et Cie, Paris, 1967).